Molecular Crystals and Liquid Crystals
Publication details, including instructions for authors and subscription information:
http://www.tandfonline.com/loi/gmcl16

Optical Study of the Electric Field Induced Domains in a Twisted Nematic

K. S. Krishnamurthy [a]
[a] College of Military Engineering, Pune, 411031, India

Version of record first published: 20 Apr 2011.

To cite this article: K. S. Krishnamurthy (1986): Optical Study of the Electric Field Induced Domains in a Twisted Nematic, Molecular Crystals and Liquid Crystals, 133:1-2, 1-17

To link to this article: http://dx.doi.org/10.1080/00268948608079557

Mol. Cryst. Liq. Cryst., 1986, Vol. 133, pp. 1–18
0026-8941/86/1332–0001/$20.00/0

Printed in the United States of America

Optical Study of the Electric Field Induced Domains in a Twisted Nematic

K. S. KRISHNAMURTHY

College of Military Engineering, Pune 411031, India

(*Received August 28, 1985*)

Optical microscopic observations have been carried out on the distortions due to AC fields in a 90°-twisted nematic sample of a phenyl benzoate having a high electrical conductivity and a small, positive dielectric anisotropy. In a narrow frequency region (0–200 Hz), Williams-type domains form. The focal lines corresponding to the region of greater alignment distortion exhibit a triplet fine structure with the components showing interesting polarization characteristics. The linear domains turn wavy and increasingly complex with increase in the voltage. Above 200 Hz, a gradual transition to the frequency region of uniform bulk homeotropic reorientation takes place via a region of linear and loop domains; the threshold voltage rises steeply in the transition region.

The study also includes a discussion of the voltage variation of transient responses and changes in optical path, at different frequencies and temperatures. The rise time varies inversely as the square of the voltage, but depends both on frequency and temperature. The decay response strongly depends on the voltage, particularly near the threshold of distortion.

Keywords: optical study, twisted nematic, electric-field-induced domains

1. INTRODUCTION

Since the initial demonstration by Schadt and Helfrich[1] that a quarter-turn nematic twist cell placed suitably between a pair of polarizers could act as an electrically controllable light valve, a great deal of work has been done on the electro-optical behaviour of twisted nematic liquid crystals (TNLCs).[2] The main reason for interest in Schadt-Helfrich effect, as is well-known, has been its use in display applications.[3] Thus much of the work on TNs is on display-related aspects

of twist cells, and there are apparently no detailed reports of the salient features of regular domains in TNs. Although Raynes[4] has discussed the Williams domains texture in nematics with weak positive dielectric anisotropy ($\Delta\epsilon$), he has made no mention of the complex changes occurring in the texture at elevated voltages or the finer aspects of the state of polarization of the "domain lines;" rather the interest in the WD pattern has been to use it as a means of distinguishing the areas of reverse twist and of identifying half-turn twisted areas.

The properties of materials of practical interest are such as to produce a uniform bulk normal reorientation rather than periodic domains in the TN sample. For instance, to minimise power dissipation, the electrical conductivity (σ) should be kept low and, to have fast transient responses[5] and low threshold voltage (V_{th}),[6] the value of $\Delta\epsilon$ should be kept large. Materials with opposite properties (high σ and low $\Delta\epsilon$), although are not of value for display, might be expected to exhibit interesting domain features. In fact, we have recently observed[7] certain novel domain patterns in the π-twisted sample of a phenyl benzoate with high σ and low $\Delta\epsilon$. Briefly, this observation was made as follows: A homogeneously aligned sample of the nematic was subjected to a high enough electric field to produce turbulence in it. Upon removal of the field, regions of π-twist formed in the relaxing fluid; these regions gradually collapsed and disappeared, but showed "longitudinal" Williams domains on reimposition of the field during their presence. The domains showed complex wavy structures at elevated voltages. In order to examine if similar instabilities also occurred in the $\pi/2$-twisted configuration of the nematic, a detailed study was undertaken. The results that emerged are presented here.

2. EXPERIMENTAL

A reagent grade sample of butyl p-(p-ethoxyphenoxycarbonyl) phenyl carbonate (BPC)

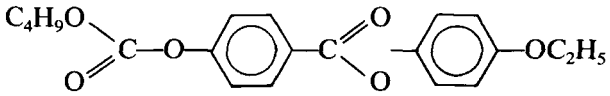

supplied by Eastman Organic Chemicals was used without further purification. It showed a reversible nematic phase between *ca.* 55°C and 85°C. The value of $\Delta\epsilon$ of BPC has been found[8] to vary from

about 0.21 at 55°C to 0.06 at 84°C. The static conductivity of BPC, as estimated from current-voltage measurements, was of the order of $10^{-8}\ \Omega^{-1}\ cm^{-1}$ in the nematic region. The sample cell configuration was as shown in Figure 1. The electrode surfaces were rubbed in perpendicular directions. They were separated by a teflon spacer of thickness 75 μm. The cell was housed in a hot-stage that could be maintained at the desired temperature to an accuracy of ±0.1°C. The textures were examined in transmitted light under a Carl Zeiss polarizing microscope.

3. RESULTS AND DISCUSSION

A. Optical textures

In the field-free state, the sample was divided into regions of reverse twist[4] (S_1 and S_2, Figure 1), demarcated by thin boundary lines. The following description of the domain patterns refers to those observed in the region S_1, in white light, at 75°C and 100 Hz. Reference directions are given in Figure 1. Voltages stated are rms values.

As the voltage applied to the sample (V) was gradually increased, the distortion pattern was first observed at about 7 V (which is considerably higher than the threshold voltage estimated from birefringence studies, as will be discussed in Sec. 3D). The pattern was that of Williams domains (WD), consisting of regularly spaced striations extending along y'. As could be expected,[9] the focal lines due to the domains were clearly seen in ordinary light, but a better contrast was obtained when the incident light was polarized along x (Figure 2(a)). However, unlike in the case of the usual WD pattern, the focusing action of the fluid did not totally disappear for the ingoing waves polarized along y and this aspect will be discussed in detail later in this section.

The Williams domains observed in the TN samples of BPC differed from those observed in the planar (i.e. homogeneously aligned) samples of BPC[10] in some ways: In the first case, the domains were straight at the threshold voltage and remained stable at higher voltages. In the second case, the domains were initially zig-zag and became oscillatory at higher voltages, eventually giving way to turbulence. More significantly, perhaps, no dust particle motion was discernible in the TN case, whereas a periodic oscillatory motion of dust particles, indicative of fluid-circulation about the axes of domains, was observable in the planar nematic case.

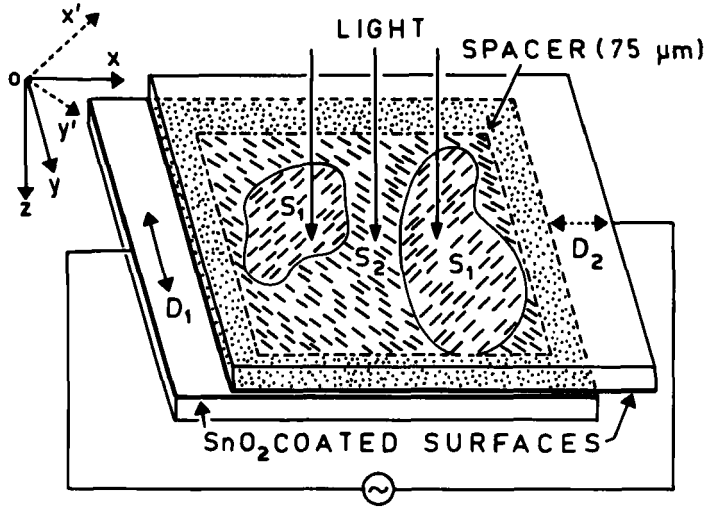

FIGURE 1 Experimental arrangement for observing the domains in twisted nematic BPC. D_1 and D_2 are the directions of molecular alignment at the bottom and top electrode surfaces. S_1 and S_2 are the regions of reverse twist showing the initial director-orientations in the midplane. In the orthogonal reference frames xyz and $x'y'z$, x' and y' are at 45° to x and y.

The finer features of the texture in Figure 2(a) are as follows: The real images, which are the alternate thinner lines formed by the convergence of light waves passing through the regions of minimum distortion and emerging polarized along y, are without any structure. In contrast, the virtual images, which are the alternate thicker lines formed by the waves diverging through the regions of greater distortion, consist of two closely-spaced components. The stronger and weaker of these components are due to the waves which after emergence are polarized along y and x, respectively. This is shown by the extinction of the weaker component and the presence of the stronger, when the field is viewed through an analyser (A) with its axis along y (Figure 2(b)). This implies that the "wave guide" effect of the nematic is present for the stronger component, but not for the weaker. Therefore, the light responsible for the weaker component must be passing through the regions of maximum bulk homeotropic reorientation (where the adiabatic approximation[11] fails), while the light giving rise to the stronger component must be passing through the neighbouring regions (where the approximation still holds good).

In the usual WD instability in homogeneously aligned samples, the molecules undergo periodic bend type reorientations in the plane of the director and the field.[9] But the reorientation in a TN would

involve all the three types of elastic deformations, i.e., the splay, twist and bend deformations.[2] As a result, the domain pattern will not be completely extinct for the ingoing wave polarized along y. Thus in Figure 2(c), while the real images are absent, the focal lines are seen in the regions of greater distortion. The bright line-images in the Figure are considerably separated from their corresponding shadow lines, signifying a large sideward deviation of the light waves forming them. Further, the dark-bright and bright-dark sequence of the lines is indicative of the opposite sense in which the directors tilt successively.

The focal lines in Figure 2(c) disappear on insertion of the analyser with its axis along x (Figure 2(d)). Thus they are formed by the light traversing through regions of maximum distortion and no optical activity. These lines were in focus in the plane of virtual images indicating that for the light vibrating along y, the region of maximum reorientation is optically less dense than the neighbouring regions. But for its focal power, therefore, the region of near-normal alignment behaves much like a Wollaston prism in that it separates the x and y components of the incident light vector sideways. The sequence of this separation alternates along the x-direction due to the alternation in the sense of director rotation.

From these observations, it may be inferred that, when the incident light vector has both the x and y components, the pattern should consist of (i) a set of real focal lines due to the x-component of the incident light emerging polarized along y (I^r_{xy}), (ii) a set of virtual images due to the y-component of the incident light emerging polarized along y (I^v_{yy}) and (iii) two other sets of virtual line-images, both due to the incident x-component of light, but one caused by the outgoing waves vibrating along x (I^v_{xx}) and the other by those vibrating along y (I^v_{xy}). In natural light, the virtual images were broad and unresolved. But in support of our conclusions it may be mentioned that (a) when only an analyser oriented along y was used, the pattern consisted of the succession of bright lines: I^r_{xy}, $I^v_{xy} - I^v_{yy}$, I^r_{xy} ..... (texture appearing similar to that in Figure 2(a)), and (b) when only an analyser set along x was used, the texture was of a succession of images I^v_{xx}, looking like that in Figure 2(c), but with the dark and bright lines interchanged.

The domains underwent increasingly complex changes with increase in voltage. Initially, the real focal lines I^r_{xy} turned wavy and the virtual lines I^v_{xy} developed wedge-like sideward extensions around which the wavy lines smoothly curved (Figure 2(e)). The "wave guide" action of the structure was still present in the region of wavy lines as

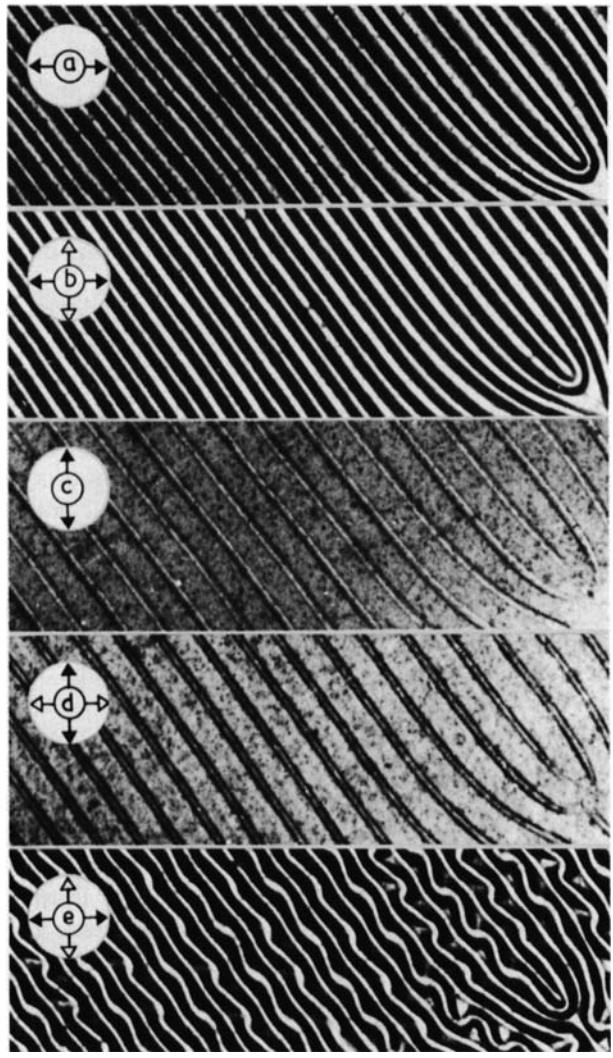

FIGURE 2 Distortion patterns observed in BPC at 75°C and 100 Hz. The field of view corresponds to the region S_1 in Figure 1, so that the diagonal focal lines are along y' and the horizontal and vertical directions along x and y. The arrows with solid and open triangular heads indicate the settings of the polarizer and analyser, respectively. Figures (a)–(g) show the same region of the sample while (h)–(j) show different regions. Voltages are: (a)–(d) 9.7 V, (e) and (f) 14.1 V, (g) 17.0 V, (h) 17.5 V, (i) 18.0 V and (j) 22.2 V. The period of the real or virtual images (that is, for example, the distance between the alternate bright lines in Figure (a)) is *ca.* 65 μm in all cases.

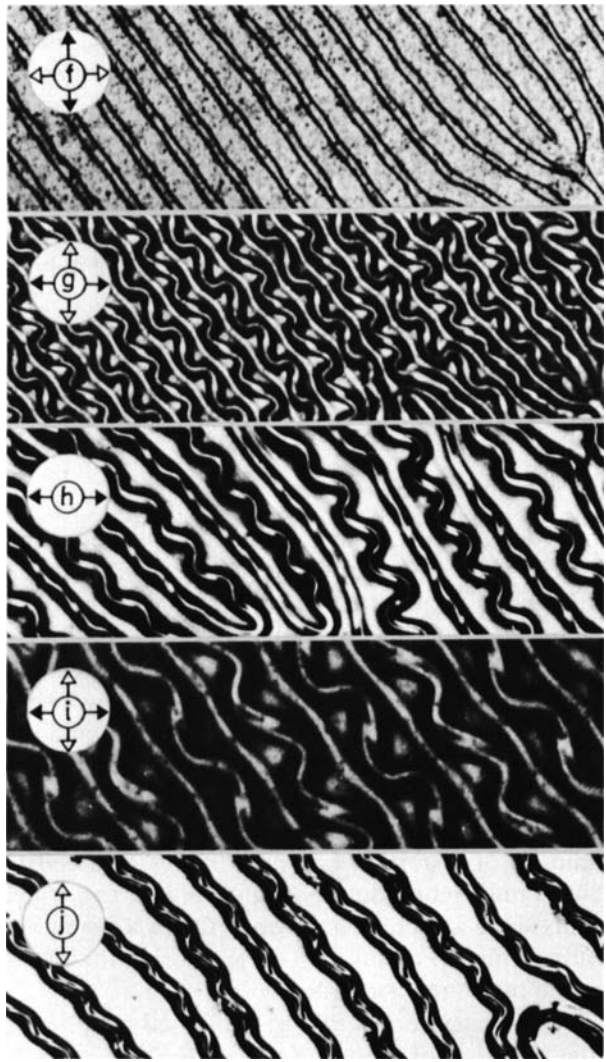

FIGURE 2 (Continued)

these lines were not observed for P along y and/or A along x (Figure 2(f)). At about 17 V, the wavy lines were seen to broaden slightly and periodically at one-wavelength interval, indicating a fine structure (Figure 2(g)). The structure clearly revealed itself as zig-zag triplet formations at *ca.* 18 V (Figures 2(h) and 2(i)). At about 22 V, the

virtual images completely disappeared showing that near-complete homeotropic orientation had taken place in the areas of their original occurrence. The regions of real images then reduced into walls between the normally aligned regions. Figure 2(j) shows the walls with their focal images which possess a well-resolved triplet structure. Similar focal line patterns have been observed earlier[12] due to the walls formed in the dielectric regime of initially homogeneously aligned samples of BPC. It may be added that, while TN samples never showed turbulence, planar samples showed turbulence at higher voltages in the low frequency region.[10]

The complex textures in Figures 2(e)–(j) are similar to the textures observed in the half-turn twisted samples of BPC.[7] These textures are significantly different from the sinusoidal wavy patterns exhibited by MBBA,[13] as explained in Ref. 7.

B. Domains in monochromatic light

The dynamical behaviour of the fluid in the low frequency region (upto *ca.* 500 Hz) could be visually followed by means of interference fringes upto voltages of about 2.5 V_{th}. The fringes were observed in mercury green light by placing the sample between crossed polarizers with their transmission axes at 45° to the molecular alignment directions at the substrates. The textural sequence following the application of a low frequency field is schematically represented in Figure 3. Initially, after the application of the field, the extinction of light showed up in various parts of the visual field, indicating non-uniform distortion in the sample mid-plane. The fringes gradually enlarged with the build up of distortion and new fringes emerged from the regions of maximum reorientation (Figure 3(a)). The fringes from different points along y' merged in time and finally a system of straight parallel bands formed (Figures 3(b)–(d)). During the decay, these events occurred in the reverse order.

In the high frequency region (>1 kHz), closed fringe systems appeared at the locations of loop domains as in the case of homogeneously aligned samples.[12] In the transition region (200–1000 Hz), some areas showed the fringes of the type in Figure 3 and the others, the fringes due to loop domains.

C. Frequency variation of the voltage threshold

It has long been known[2,14] that the "wave guide" effect of the TN structure for the incident light vector along x or y disappears significantly above the deformation potential, V_D. Thus, when the cell is

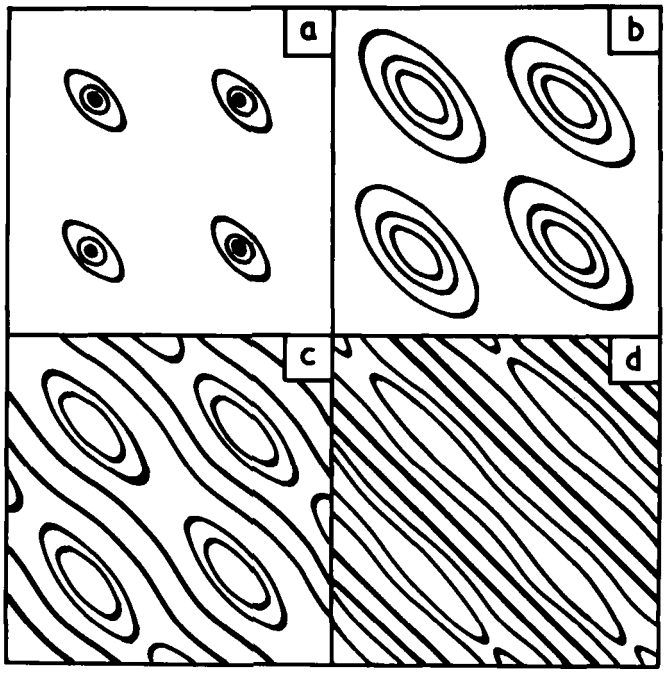

FIGURE 3 Schematic representation of the changes in interference pattern observed during the growth of domains in a region such as S_1 of Figure 1. The fringes spread out from the regions of maximum alignment distortion.

between two polarizers with their axes along x and/or y, the transmitted intensity begins to change sharply at a potential (the optical threshold, V_O, which is higher than V_D by an amount that increases with the sample-thickness.[2] V_D is determined from changes in the cell capacity[14] or the sample birefringence.[15]

The threshold voltage, V_{th}, for BPC was estimated visually from the changes in birefringence. As mentioned in Sec. 3B, BPC showed fringes rather than a uniform illumination in the visual field. The voltage at which the interference effects just began to appear was taken as V_{th}. Evidently V_{th} does not represent either V_O or V_D, but is likely to be of an intermediate value.

It should be mentioned that V_{th} had a lower value in areas of disturbed molecular alignment (voids, dust particles, disclinations etc.); the fringes were first observed in such areas. Our measurements pertain to regions relatively free from disturbances.

Figure 4 shows the frequency variation of V_{th} at 66°C and 76°C. The general decrease of V_{th} at 76°C implies a decrease in $K/\Delta\epsilon$ (K being the effective elastic constant) with rise in temperature; a similar

behaviour has been observed in some other cases.[16] On the basis of the textures seen, three frequency regions have been distinguished. In the region A (0–200 Hz), where V_{th} rises slowly with frequency (f), the textures observed were those illustrated in Figure 2. In the region B, extending upto about a kHz at 66°C and 1.5 kHz at 76°C, where V_{th} rapidly rises with f, the threshold textures showed both Williams domains and loop domains, the latter becoming more prominent at higher frequencies. At lower frequencies, the loops were longish, more elongated in the directions y' and x' in the regions S_1 and S_2 respectively (Figure 1). The loops had a general tendency to

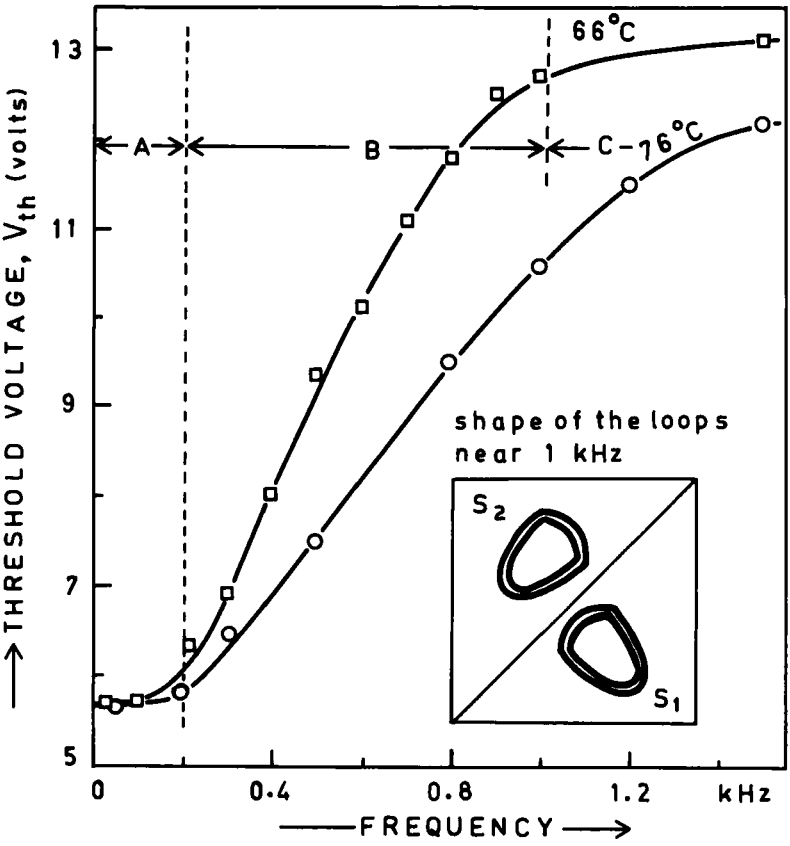

FIGURE 4 Dependence of threshold voltage on frequency. In the region A the type of distortions shown in Figure 2 are observed. Region C is the dielectric regime showing normal reorientation and walls. Region B is the transition region between the regions A and C. The inset shows, schematically, the type of loop domains observed at higher frequencies in the areas of reverse twist S_1 and S_2.

collapse and disappear. At higher frequencies (near 1 kHz), the collapsing domains had a characteristic unsymmetrical appearance (when compared with the loop domains in planar samples[12]) illustrated in the inset of Figure 4. The rate of collapse of the loops increased with V. At higher voltages (*ca.* 25 V); the focal line of the loop walls showed a zig-zag structure, just as the loop walls in homogeneously aligned samples of BPC.[12]

In the region C, at the threshold, some loop domains and open walls formed initially; the loops disappeared in time while the open walls endured.

D. Transient responses

In a field effect experiment, a sudden application (or removal) of the field is expected to bring about an exponential growth (or decay) of the director distortions.[5] The expressions for the time constants T_r and T_d characterising the rise and decay in a twist cell are given by[5]

$$T_r^{-1} = \frac{\epsilon_0 \Delta\epsilon}{\eta d^2}(V^2 - V_{th}^2) \tag{1}$$

$$T_d = \frac{\eta d^2}{K\pi^2} \tag{2}$$

where η is the average viscosity, d the sample thickness, K the effective elastic constant and ϵ_0 the permittivity of free-space; V_{th} and K are, in turn, given by[6]

$$V_{th} = \pi\sqrt{\frac{K}{\epsilon_0\Delta\epsilon}} \quad \text{and} \quad K = K_{11} + \frac{1}{4}(K_{33} - 2K_{22}).$$

Here K_{ii} are the Frank elastic constants.

The response times are, in practice, determined by measuring with a photocell the intensity of the light transmitted by the cell placed suitably between two parallel or crossed polarizers. The time for a change in intensity by 90% of the final value is the total rise time τ_r or decay time τ_d, depending on the growth or decay.[17] It may be noted that τ_r and τ_d might represent T_r and T_d only approximately since light transmission may not vary proportionately with the distortion.[18]

For twist cells of practical interest τ_r and τ_d are necessarily very small (100 ms or less). But for the samples of BPC, the responses

were very slow (due to large d and small $\Delta\epsilon$), so that a rough estimate of the rise and decay times could be made by a direct visual observation of the growth and decay of interference fringes. Thus, the time taken, after switching the field on, for the steady pattern to establish was treated as the rise time, t_r. Similarly, the time for complete disappearance of the fringes after removal of the field was taken as the decay time, t_d. Evidently t_r and t_d cannot be correlated with the conventional response times τ_r and τ_d, but may be taken as rough measures of T_r and T_d (Eqs. (1) and (2)).

Figure 5 shows a plot of t_r^{-1} vs. V^2 with temperature and frequency as the parameters. The variation of t_r^{-1} is linear and fits the expression

$$t_r^{-1} = C\,(V^2 - V_{th}^2) \tag{3}$$

where C and V_{th} are functions of both temperature and frequency. The general increase in t_r^{-1} with temperature at a given frequency (plots for 66°C and 76°C at 50 Hz, Figure 5) is understandable since C includes $\Delta\epsilon/\eta$ which ratio could decrease with increase of temperature. Similarly, the slight decrease in V_{th} on increase of temperature (66°C to 76°C) could be ascribed to changes in K and $\Delta\epsilon$.[16] The role of frequency in altering the values of C and V_{th} is less obvious. The dielectric relaxation frequency of $\epsilon_\parallel$ for BPC is too large (0.4 MHz at 59°C) to expect significant changes in $\Delta\epsilon$ in the low frequency region.[8] The frequency dependence of C and V_{th} are possibly due to the high electrical conductivity of BPC. In fact, Eq. (1), derived by considering the dielectric, elastic and viscous torques, applies strictly to insulating nematics showing no regular domains. But for conducting nematics in which space charge effects are present, frequency dependence of C and V_{th} (Eq. 3) is not unexpected.

It may be mentioned that the values of V_{th} indicated in Figure 5 are lower by 10–20% when compared with their corresponding values in Figure 4. As already clarified in Sec. 3C, V_{th} in Figure 4 is likely to be between the optical and deformation thresholds; values of V_{th} in Figure 5 seem closer to the deformation threshold.

Regarding the decay process, it is predicted to be governed only by the material parameters and not the voltage prior to switch off (Eq. 2). Experimentally, τ_d is known to depend on V at all voltages.[18–20] Baise and Labes[19] ascribe the slight, linear increase of τ_d with V in certain Schiff base mixtures to turbulence arising from ionic impurities. More recently, Nakano et al.[20] have reported that, in some Schiff base derivatives, τ_d changes strongly with V, especially for smaller Vs. To fit their data, they propose the phenomenological expression:

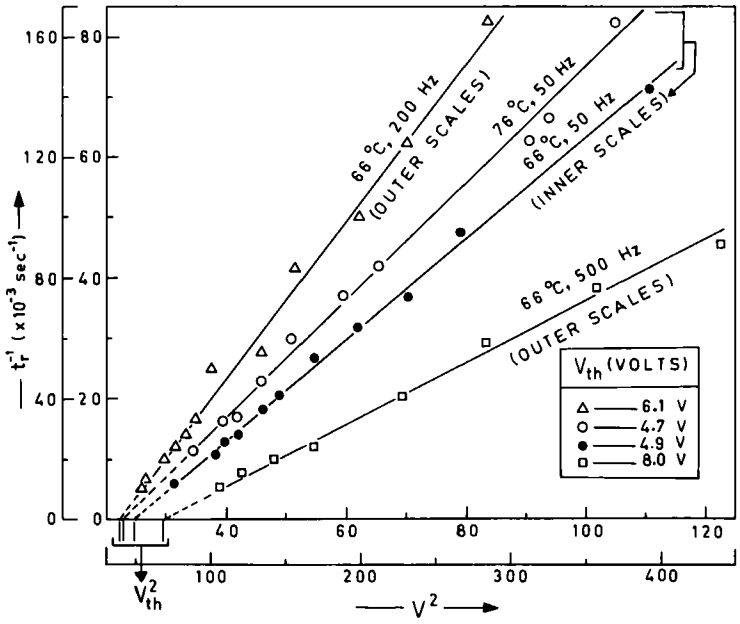

FIGURE 5 Voltage dependence of the rise response in BPC for different frequencies and temperatures; t_r is the time in which the interference pattern in the region of domains becomes completely established after a sudden application of the voltage.

$$\tau_d = \frac{\eta d^2}{\pi^2 K}\left(\frac{V}{V_{th}} - 1\right)^a \tag{4}$$

where the exponent a varies between 0.24 and 0.5 depending on the substance.

The value of t_d in BPC increased with V upto about 7–9 V, but thereafter remained either constant or decreased slightly (Figure 6). Switch off from higher voltages could improve the decay response because of "backflow" (or a temporary initial increase in director distortion in the sample-midplane) causing a nonexponential, oscillatory decay.[21] The pronounced dependence of t_d on V at lower voltages can only be attributed to high ionic conduction in BPC. The curves in Figure 6, on the whole, are not consistent with Eq. (4), although a small region of consistency (linearity) exists for intermediate voltages. The slopes in the linear region, interestingly, are about 0.4, as in Eq. (4).

Figure 6 also shows that t_d, at a given V, is dependent on both frequency and temperature. The decrease of t_d with rising temperature shows that the decay response is primarily due to the viscosity

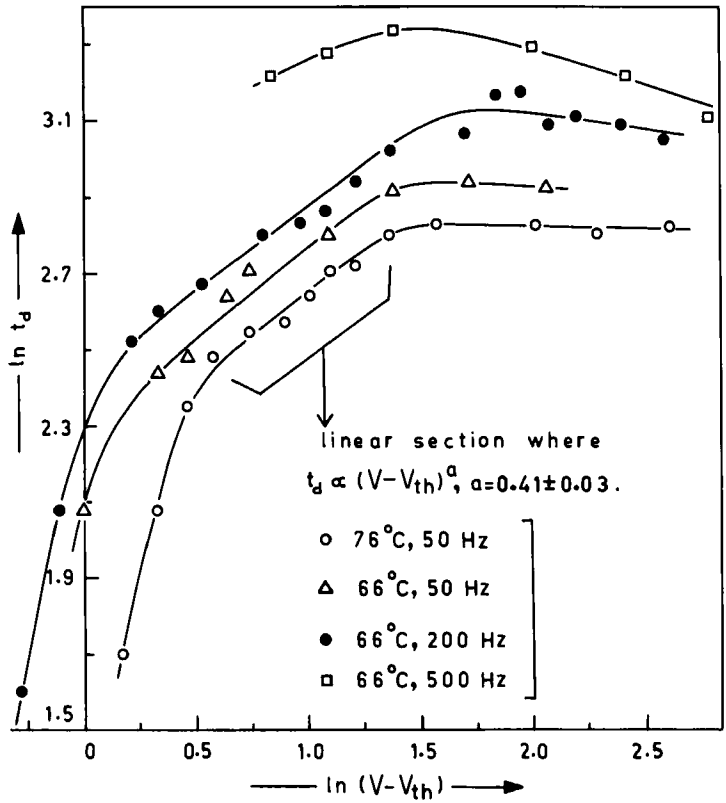

FIGURE 6 Voltage dependence of the decay response in BPC for different temperatures and frequencies; t_d is the time in which the interference pattern due to the distorted sample completely disappears after switch off. The V_{th} values are from the rise response plots of Figure 5. The curves represent the phenomenological expression for decay response in Ref. 20 (Eq. 4, text) in the region of linearity.

and secondarily to the elastic constant. Similar behaviour has been reported for some other TNs.[16,22] As in the case of t_r, the reason for change in t_d with frequency may have to do with the high conductivity of the material.

E. Voltage dependence of maximum path change

The slow build up of alignment deformation over a considerable range of voltages enabled a direct estimation of the maximum decrease of optical path (Δ) as a function of V. For this purpose, the number of interference fringes emerging in the regions of maximum distortion (Sec. 3B) were counted and from the average of several trials in different well aligned areas Δ was computed. The Δ so determined

will of course be approximate to the extent that the initial and final fractional orders of interference cannot be known with certainty. This error is less serious when Δ is large (at higher voltages) than when it is small (near V_{th}).

Figure 7 shows the variation of Δ with V for different frequencies and temperatures. The curves corresponding to 66°C and different frequencies show that the effect of field strength in causing disalignment decreases markedly with increasing frequency. At 50 Hz, the curve corresponding to 76°C practically follows that for 66°C upto about 6.5 V, but thereafter assumes a lower trajectory. At higher

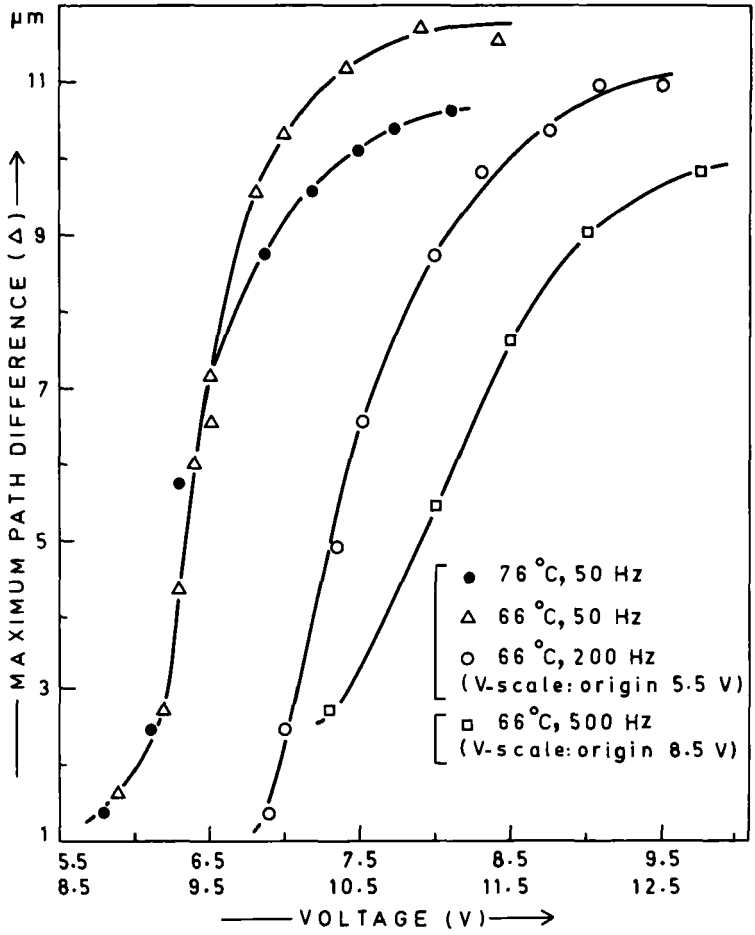

FIGURE 7 Maximum change in optical path as a function of voltage at different temperatures and frequencies as estimated from interference fringes.

temperatures, the extent of bulk homeotropic orientation may be expected to be more due to a general decrease of elastic forces (as evidenced by a decrease in V_{th} (Figure 4). But, concomitantly, the birefringence of the fluid decreases. Hence Δ may be less at higher temperatures and no general conclusion on the nature of variation of Δ with temperature seems possible.

Acknowledgments

I am grateful to the Commandant, College of Military Engineering, for the experimental facilities and to Dr. A. P. B. Sinha, National Chemical Laboratory, for the conducting glass plates.

References

1. M. Schadt and W. Helfrich, *Appl. Phys. Lett.*, **18**, 127 (1971).
2. V. G. Chigrinov, *Sov. Phys. Crystallogr.*, **27**, 245 (1982); H. Kelker and R. Hatz, Handbook of Liquid Crystals (Verlag Chemie, Weinheim, Deerfield, 1980), p. 127, p. 192 and pp. 616–617.
3. D. W. Berreman, in Nonemissive Electrooptic Displays, edited by A. R. Kmetz and F. K. von Willisen (Plenum Press, New York and London, 1975), p. 9; P. A. Penz, *Proc. S.I.D.*, **19**, 43 (1978); E. P. Raynes, *IEEE Trans. Electr. Dev.*, **26**, 1116 (1979).
4. E. P. Raynes, *Electron. Lett.*, **9**, 101 (1973); ibid **10**, 141 (1974).
5. E. Jakeman and E. P. Raynes, *Phys. Lett.*, **39A**, 69 (1972); F. Brochard, P. Pieranski and E. P. Guyon, *Phys. Rev. Lett.*, **28**, 1681 (1972).
6. F. M. Leslie, *Mol. Cryst. & Liq. Cryst.*, **12**, 57 (1970); C. J. Alder and E. P. Raynes, *J. Phys. D.*, **6**, L33 (1973); H. J. Deuling, *Mol. Cryst. & Liq. Cryst.*, **27**, 81 (1974).
7. K. S. Krishnamurthy and M. S. Bhate, *Jpn. J. Appl. Phys.*, **24**(5), 512 (1985).
8. W. H. de Jeu and Th. W. Lathouwers, *Mol. Cryst. & Liq. Cryst.*, **26**, 225 (1974).
9. P. A. Penz, *Phys. Rev. Lett.*, **24**, 1405 (1970).
10. K. S. Krishnamurthy, *Jpn. J. Appl. Phys.*, **23** (9), 1165 (1984).
11. S. Chandrasekhar, Liquid Crystals (Cambridge University Press, Cambridge, 1977), p. 195.
12. K. S. Krishnamurthy and M. S. Bhate, *Mol. Cryst. & Liq. Cryst.*, **128**, 29 (1985).
13. S. Kai and K. Hirakawa, *J. Phys. Soc. Jpn.*, L **40**(1), 301 (1976).
14. C. J. Gerritsma, W. H. de Jeu and P. van Zanten, *Phys. Lett.*, **36**, 389 (1971).
15. M. F. Grebenkin, V. A. Seliverston, L. M. Blinov and V. G. Chigrinov, *Sov. Phys. Crystallogr.*, **20**, 604 (1975).
16. F. H. Kahn and R. A. Burmeister Jr., in Nonemissive Electrooptic Displays, edited by A. R. Kmetz and F. K. von Willisen (Plenum Press, New York and London, 1975), p. 289.
17. T. S. Chang, P. E. Greene and E. E. Loebner, in Liquid Crystals and Ordered Fluids, edited by J. F. Johnson and R. S. Porter (Plenum Press, New York, 1974), Vol. 2, p. 115.
18. C. S. Bak, K. Ko and M. M. Labes, *J. Appl. Phys.*, **46**, 1 (1975).
19. A. I. Baise and M. M. Labes, *Appl. Phys. Lett.*, **24** (7), 298 (1974).

20. F. Nakano, H. Kawakami, H. Morishita and M. Sato, *Jpn. J. Appl. Phys.*, **19**, 659 (1980).
21. C. J. Gerritsma, C. Z. van Doorn and P. van Zanten, *Phys. Lett.*, **48A**, 263 (1974); D. W. Berreman, *J. Appl. Phys.*, **46**, 3746 (1975).
22. J. W. Park and M. M. Labes, *J. Appl. Phys.*, **48**, 22 (1977); H. A. Tarry, *Electron. Lett.*, **11**, 339 (1975).